# Phase-Plane Approach to Nonlinear Propagation in Dielectric Slab Waveguide

Tullio Rozzi, *Fellow, IEEE,* Franco Chiaraluce, and Leonardo Zappelli

*Abstract*—**Considerable interest is currently being devoted to nonlinear propagation in dielectric slab waveguides for integrated optics and millimetric applications. Apart from a few specific analytical cases, much of the current work is numerically based, so that the qualitative features of the solutions are lost. In this contribution, we look at on the problem in the framework of a phase-plane approach, prior to seeking numerical solutions by, say, the Runge–Kutta method. As a result, qualitative aspects, such as "integrals of motion" in phase-plane do emerge from the analysis. Systematic consideration of these quantities narrows the range of possible solutions down whilst providing direct physical interpretation of the same. Particularly suggestive, in this respect, are the interpretations of the appearance of higher order modes and of the energy/boundary conditions constraints typical of the nonlinear problem. The approach is quite general and results will be shown in the TE and TM cases.**

## I. Introduction

IT HAS been apparent for a long time that nonlinear propagation in optical and millimetric waveguides holds promise in the context of integrated signal processing [1]–[2]. In recent years, with the development of technology, increasing attention has been devoted to these effects with a view to realizing optically bistable devices, switchers, upper and lower threshold devices, optical limiters and so on [3]–[5]. In spite of the interest generated by this wide range of potential applications, much work still remains in order to achieve an effective characterization. Only a few cases can be treated analytically. Among them, the most important is certainly that of the TE-polarized waves propagating in media with Kerr-like nonlinearity [6]–[8]. In all other cases numerical methods, such as finite elements [9], Runge–Kutta [10], beam propagation [11], must be employed. While generally effective, these methods present the disadvantage of not allowing physical interpretation of the solutions. In nonlinear problems, in fact, particularly important is the existence and identification of invariant quantities related to "observable" physical parameters of the configuration, such as energy. Using purely numerical methods, however, a qualitative analysis of the structure is not possible and many of its underlying features can not be perceived.

Manuscript received December 10, 1990; revised May 29, 1991.

The authors are with the Dipartmento di Elettronica ed Automatica, Università degli Studi di Ancona, Via Brecce Bianche, 60131 Ancona, Italy.

IEEE Log Number 9102819.

The aim of the present paper is to overcome some of these limitations by means of an approach that, although numerical in itself, is led by a qualitative analysis in phase-plane. The latter is a representation well known in the theory of nonlinear first-order systems [12], but still practically unused in the solution of electromagnetic problems. Nevertheless, as will be shown, its use affords a number of important advantages: first of all, a great reduction of the computer time required in the analysis, as this is guided by a qualitative preliminary investigation that narrows the range where solutions can be found. Subsequently, there emerges a simple and complete physical interpretation of the results obtained by the numerical computations. In particular, it is possible to highlight the role of some "integrals of motion" occurring in phase-plane: in fact, these are quantities that identify a set of modes for a given energy level in phase-plane.

The method is completely general and can be applied to every situation, including arbitrary profiles of the linear permittivity and arbitrary types of nonlinearity, both for TE and TM modes.

## II. Theory: TE-Case

The nonlinear dielectric slab structure to be analyzed is shown in Fig. 1. It consists of a thin, optically nonlinear, dielectric film, sandwiched between semi-infinite linear dielectrics. Restricting ourselves to TE polarization, the electric field $E_y$, propagating along the $z$ axis as exp $[-j(\beta z - \omega t)]$, must satisfy, in the three regions, the following equations (subscript $i = 1, 2, 3$ is used to label the media, as in Fig. 1):

$$\frac{d^2E_{y1}}{dx^2} + (k_0^2\epsilon_1 - \beta^2)E_{y1} = 0 \qquad -\infty < x \le -d \tag{1a}$$

$$\frac{d^2E_{y2}}{dx^2} + (k_0^2\epsilon_2 - k_0^2\tau|E_{y2}|^\alpha - \beta^2)E_{y2} = 0 \qquad -d \le x \le +d \tag{1b}$$

$$\frac{d^2E_{y3}}{dx^2} + (k_0^2\epsilon_3 - \beta^2)E_{y3} = 0 \qquad +d \le x < +\infty \tag{1c}$$

where $k_0 = 2\pi/\lambda$ is the wavenumber in the free space and $\lambda$ is the wavelength. Our attention will be centered on a defocusing nonlinearity so that, in (1b), $\tau > 0$.

It is useful to introduce some normalizations. First of all, we can multiply the above expressions by the factor

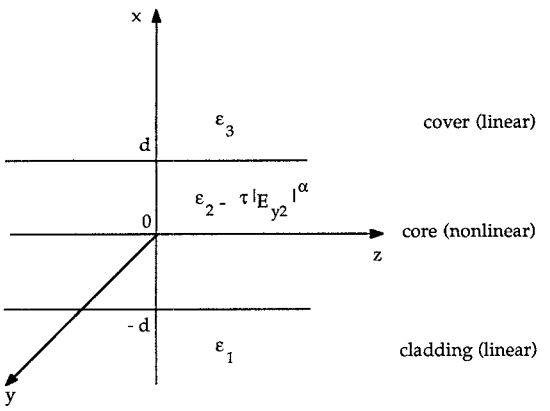


Fig. 1. Asymmetric nonlinear waveguide with nonlinear core and linear cladding and cover layers.

$\tau^{1/\alpha}/k_0^2$ and define the following normalized quantities:

$$t = k_0 x \tag{2a}$$

$$b = \frac{\beta}{k_0} \tag{2b}$$

$$a = k_0 d \tag{2c}$$

$$u_i = \tau^{1/\alpha} E_{yi} \qquad i = 1, 2, 3. \tag{2d}$$

Substituting these variables in (1a)–(1c), the wave equations can be rewritten as

$$u_1'' - k_1^2 u_1 = 0 \qquad -\infty < t \leq -a \tag{3a}$$

$$u_2'' + (k_2^2 - |u_2|^\alpha) u_2 = 0 \qquad -a \leq t \leq +a \tag{3b}$$

$$u_3'' - k_3^2 u_3 = 0 \qquad +a \leq t < +\infty \tag{3c}$$

where

$$k_i = \sqrt{b^2 - \epsilon_i} \qquad i = 1, 3 \tag{4a}$$

$$k_2 = \sqrt{\epsilon_2 - b^2} \tag{4b}$$

and the apex $'$ denotes a differentiation with respect to $t$.

The nonlinear equations system (3a)–(3c) can be efficiently represented and studied in a so called "phase-plane." In such a plane, the relationship between $u_i$ and its first derivative $u_i'$ is described, as a function of $t$, by some curves which must be continuous in correspondence of the interface abscissae $t = \pm a$. More precisely, (3a) holds in the cladding region with the following, obvious, asymptotic conditions:

$$u_1(-\infty) = u_1'(-\infty) = 0 \tag{5}$$

so that, integrating with respect to $u_1$ between $u_1(-\infty)$ and $u_1(t)$, we have

$$u_1 = u_{10} \exp [k_1(t + a)] \tag{6}$$

and

$$v_1 \equiv u_1' = k_1 u_1. \tag{7}$$

Quite similar expressions hold, of course, in the cover region, where we obtain

$$u_3 = u_{30} \exp [-k_3(t - a)] \tag{8}$$

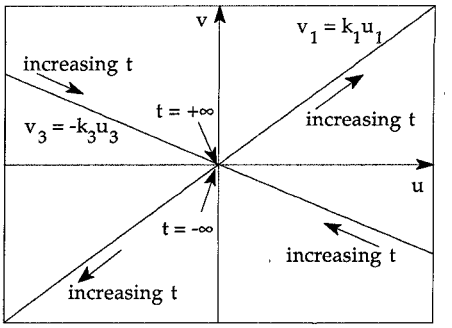


Fig. 2. Sketch, in the phase-plane, of the representation of the locus equations for the linear cladding and cover layers.

and

$$v_3 \equiv u_3' = -k_3 u_3. \tag{9}$$

Starting from (7) and (9), the relationship between the normalized field $u_i$ and its first derivative $v_i (i = 1, 3)$ in the external regions can be represented, in a plane $u$, $v$ (phase-plane) by two straight lines passing through the origin. Each point of these lines corresponds to a particular value of $t$ as well as to a particular pair of values $u_i$, $v_i (i = 1, 3)$. The orbits so described are drawn in Fig. 2, where their directions for increasing $t$ have been also evidenced, for clarity.

In particular, if we consider the fundamental mode only, assuming $u_{10} > 0$, we must select:

1) the path in the first quadrant which, starting from the origin (where $u_1(-\infty) = v_1(-\infty) = 0$), goes on the straight line $v_1 = k_1 u_1$, in the sense of increasing $t$, towards the point $[u_1(-a), v_1(-a)]$ corresponding to the core-cladding interface field;

2) the path in the fourth quadrant which, starting from the point $[u_3(+a), v_3(+a)]$, corresponding to the core-cover interface field, goes on the straight line $v_3 = -k_3 u_3$, in the sense of increasing $t$, towards the origin (where, again, we have $u_3(+\infty) = v_3(+\infty) = 0$).

The analysis can now proceed with the derivation of the paths relative to the nonlinear core. The following boundary conditions hold:

$$u_2(-a) = u_1(-a) \tag{10a}$$

$$u_2(+a) = u_3(+a) \tag{10b}$$

$$u_2'(-a) = u_1'(-a) \tag{10c}$$

$$u_2'(+a) = u_3'(+a). \tag{10d}$$

We can integrate (3b), with respect to $u_2$, between the normalized values $u_0 \equiv u_2(t_0)$ and $u_2 \equiv u_2(t)$. Noting that $\int u''\, du = \int u'\, du' = \frac{1}{2} u'^2$, we obtain the following locus on the $uv$-plane:

$$v_2^2 + u_2^2 \gamma_2 - \frac{2}{\alpha + 2} u_2^2 |u_2|^\alpha = v_0^2 + u_0^2 \gamma_2 - \frac{2}{\alpha + 2} u_0^2 |u_0|^\alpha \tag{11}$$

where $\gamma_2 = k_2^2$.

It is explicitly noted that the physical interpretation of (11) is that of an "integral of motion" in phase-plane, as in classical mechanics.

The application of these concepts to the nonlinear slab problem is further illustrated by the following considerations.

In order to describe an "allowed orbit," we can choose as an initial point $(u_0, v_0)$ the intersection of this locus with the path (7) describing the field in the cladding, i.e.,

$$v_0 = k_1 u_0. \tag{12}$$

Substitution of (12) in (11) gives

$$v_2^2 + u_2^2\gamma_2 - \frac{2}{\alpha + 2} u_2^2|u_2|^\alpha = u_0^2 (\epsilon_2 - \epsilon_1) - \frac{2}{\alpha + 2} u_0^2|u_0|^\alpha \tag{13}$$

which analytically represents the curve we are looking for. Its shape depends, of course, on the exponent $\alpha$, whose value controls the strength of the nonlinearity; for example, in the trivial case of $\alpha \to -\infty$, the nonlinearity disappears and the curve is reduced to an ellipse.

Equation (13) gives not one but a family of curves (orbits), all symmetrical with respect to the $u$-axis, having $\gamma_2$ as a parameter. In particular, when $\alpha = 2$ (corresponding to a Kerr-like nonlinearity) the loci assume the shape shown in Fig. 3 where different values of the interface field, $E_y(-d)$, have been considered.

From the wave equation in the core region (3b) we infer that the following condition must be satisfied, in order to recover guided modes

$$\gamma_2 - |u_2|^\alpha > 0. \tag{14}$$

Equation (14) delimits the portion of the $uv$-plane where guided modes can be found. Furthermore, only one orbit is capable of reaching the limit condition $|u_{2\max}| = \gamma_2^{1/\alpha}$, where $|u_{2\max}|$ is the maximum value for the modulus of the normalized field resulting from the intersection of the orbit (13) with the $u$-axis.

The orbit passing through $u_{2\max}$ can be determined simply by assuming, as starting point in (11), $|u_0| = \gamma_2^{1/\alpha}$, $v_0 = 0$. For example, in the case of the fundamental mode, which is characterized by the condition $u_i \geq 0$ $(i = 1, 2, 3)$, with some algebraic manipulations, the equation of this "limit orbit" results:

$$v_2^2 + u_2^2\left(\gamma_2 - \frac{2}{\alpha + 2} u_2^\alpha\right) = \gamma_2^{(\alpha+2)/\alpha} \frac{\alpha}{\alpha + 2}. \tag{15}$$

All the orbits that represent guided modes must lie inside the limit orbit. In particular, in the case of Kerr nonlinearity, an example of significant locus is reported in Fig. 4, where also the straight lines relative to the external regions are drawn for completeness.

As regards the slope of any orbit, for the points of the $u$-axis, where $v = 0$, we have in general (for simplicity, in the following, we will omit suffix 2 when not necessary):

$$\left.\frac{dv}{du}\right|_{v=0} = \left.\frac{\dfrac{dv}{dt}}{\dfrac{du}{dt}}\right|_{v=0} = \left.\frac{u''}{v}\right|_{v=0} = \infty. \tag{16}$$

Only in the limit case $(u|_{v=0} = \gamma_2^{1/\alpha})$ we obtain, directly from the wave equation, the condition $u''|_{v=0} = 0$, which entails that the derivative $dv/du|_{v=0}$ has two finite and different values. This result is quite evident in Fig. 4. Finally, we observe that the limit value of $u$ increases when the eigenvalue $\beta$ decreases, and the region bounded by the limit orbit becomes wider and wider.

The problem of finding a guided mode becomes that of determining, along one of the orbits of Fig. 3, a path connecting the two straight lines relative to the outer layers. Among the possible paths, each of them described as $t$ varies, we have to search for the one which connects the point $[u(-a), v(-a)]$, on the straight line $v(t) - k_1 u(t) = 0$, with the point $[u(a), v(a)]$, on the straight line $v(t) + k_3 u(t) = 0$, covering, at the same time, a distance $\Delta t$ exactly equal to the normalized width of the core region, $2a$. Obviously, there may be more than one way for doing so and, according to the quadrants where start and end points lie, it is possible to obtain different solutions. Moreover, owing to the closed structure of the orbit, evident, for example, from an inspection of Fig. 3, we can

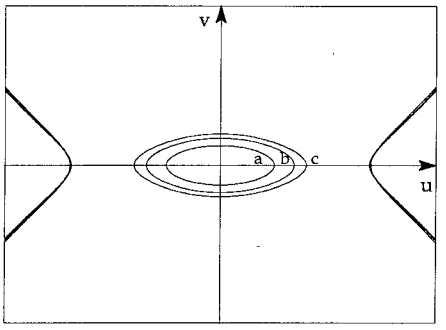


Fig. 3. Sketch, in the phase-plane, of the representation of the locus equation for the nonlinear core layer in the case of a Kerr-like nonlinearity. The interface field $E_y(-d)$ is assumed as a parameter: (a) $E_y(-d) = 0.7 \cdot 10^4$ V/m; (b) $E_y(-d) = 1.0 \cdot 10^4$ V/m; (c) $E_y(-d) = 1.2 \cdot 10^4$ V/m. $\tau$ is equal to $10^{-9}$ m$^2$/V$^2$.

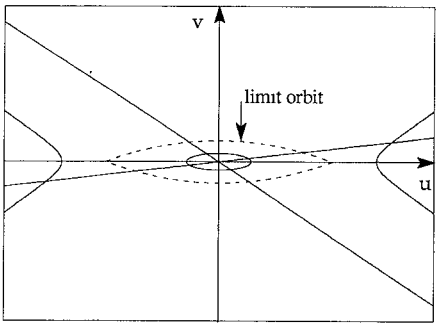


Fig. 4. Representation of the significant loci in the case of Kerr nonlinearity.

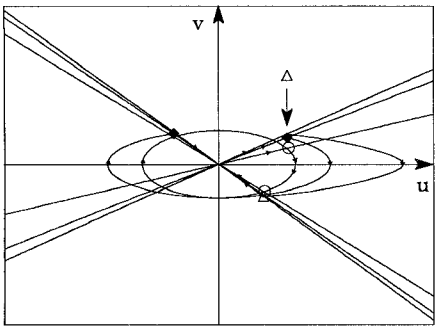


Fig. 5. Sketch of typical orbits for a guide which supports three modes. We have noted with △ the orbit described by the fundamental mode, with ♦ the orbit described by the second mode and with ○ the orbit described by the third mode, using a single row (→) to denote an orbit which is covered only once and a double row (→→) to denote an orbit which is covered twice.

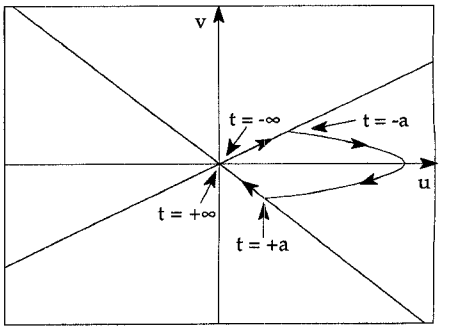


Fig. 6. Sketch of a typical orbit for the fundamental mode.

choose, as a solution, a path which makes more than one turn around the origin before reaching a point corresponding to the second dielectric interface, in any case ensuring that the covered distance is equal to $2a$. It is easy to understand that each of these possible connections corresponds to a different guided wave. In fact, together with the fundamental mode, characterized by $u > 0$, also higher order modes of order $n$, with $n = 1, 2, \cdots$, can exist, characterized by $n$ zeros of $u$ in the range $|t| \leq a$. As an example, we have plotted, in Fig. 5, typical orbits, in the case of Kerr-like nonlinearity, for a guide which supports three modes.

As regards the fundamental mode, we must consider the path that starts from the branch of the straight line laying in the first quadrant and arrives, with a clockwise rotation, to intersect the branch of the straight line laying in the fourth quadrant, making less than one full turn. In this situation, the normalized field $u$ exhibits only one maximum, whose value, as previously stressed, is reached when $v = 0$. In conclusion, the locus of interest is that qualitatively shown in Fig. 6.

Letting $v_2 = 0$ and $u_0 = \text{constant} > 0$ in the locus equation (13) and differentiating with respect to $\beta$, keeping in mind that $\gamma_2 > u_{2\max}^{\alpha}$, we have

$$\frac{du_{2\max}}{d\beta} = \frac{u_{2\max}\dfrac{\beta}{k_0^2}}{\gamma_2 - u_{2\max}^{\alpha}} > 0, \tag{17}$$

so that $u_{2\max}$ increases with $\beta$. A variation of $\beta$, for a fixed value of $u_0$, may be due to a change in some electrical or geometrical parameter of the structure. Alternatively, in a multimodal structure, when the modal order increases, the value of $\beta$ decreases, so that, for a fixed cladding-core interface field, the fundamental mode has the highest value of $u_{2\max}$, the second mode a value greater than those of all other modes except the fundamental one and so on.

Removing the constraint $u_0 = \text{constant}$, we can also investigate how the system evolves when the field at the boundary $t = -a$ varies. For such a purpose, it is necessary, first of all, to analyze the behavior of the phase constant $\beta$ as a function of $u_0$.

For the fundamental mode ($u_0 > 0$), by differentiation of the locus equation (13) with respect to $u_0$ we obtain

$$2v\frac{dv}{du_0} + 2u(\gamma_2 - u^{\alpha})\frac{du}{du_0} + u^2\frac{d\gamma_2}{du_0} - 2u_0(\epsilon_2 - \epsilon_1 - u_0^{\alpha}) = 0. \tag{18}$$

This result is valid for any value of $u$. Nevertheless it is expedient to fix the $u$-value in order to analyze the orbit variation on a straight line parallel to the $v$-axis of the phase-plane, so that we have $du/du_0 = 0$. If we put $u = u_{\max}$, $v = 0$, (18) gives

$$\frac{d\gamma_2}{du_0} = \frac{2u_0(\epsilon_2 - \epsilon_1 - u_0^{\alpha})}{u_{\max}^2}. \tag{19}$$

Obviously, the value of $d\gamma_2/du_0$ has to be the same if computed in correspondence of a different value of $u$, say $u = u^*$. Hence, also the following equation must hold

$$\frac{d\gamma_2}{du_0} = \frac{2u_0(\epsilon_2 - \epsilon_1 - u_0^{\alpha}) - 2v^*\left.\dfrac{dv}{du_0}\right|_{u=u^*}}{u^{*2}} \tag{20}$$

where $v^* = v(u^*)$. Equating the right hand sides of (19) and (20) we obtain

$$\left.\frac{dv}{du_0}\right|_{u=u^*} = \frac{u_0(\epsilon_2 - \epsilon_1 - u_0^{\alpha})(u_{\max}^2 - u^{*2})}{u_{\max}^2 v^*}. \tag{21}$$

As we have $u^* \leq u_{\max}$ and $\epsilon_2 - \epsilon_1 > u_0^{\alpha}$, $dv/du_0|_{u=u^*}$ has the same sign of the ratio $u_0/v^*$. If $u_0$ is positive, as in the present case, the locus widens as $u_0$ increases and contracts as $u_0$ decreases.

In addition, from (19) we infer

$$\frac{d\beta}{du_0} = -\frac{k_0^2}{\beta}\frac{u_0(\epsilon_2 - \epsilon_1 - u_0^{\alpha})}{u_{\max}^2} \tag{22}$$

which is always negative. So we conclude that, increasing the value of the interface normalized field $u_0$, the value of the phase constant $\beta$ decreases. As a consequence, the values of $k_1$ and $k_3$ decrease as well. This involves lower slopes for the straight lines relative to the outer regions, so that the electric field decay is slower and the field is less confined.

In conclusion, it is clear how these qualitative consid-

erations can be efficiently employed in the framework of numerical computation.

Returning now to the problem of determining a suitable path, in the sense specified above, capable of describing field propagation in the core region, this can be simply and efficiently solved by resorting to the well known Runge–Kutta method. The latter can be used in order to integrate the following system:

$$u_2' = v_2 \tag{23a}$$

$$v_2' = -(\gamma_2 - |u_2|^{\alpha})u_2 \tag{23b}$$

with initial conditions

$$u_{20} = u_1(-a), \tag{24a}$$

$$v_{20} = k_1 u_{20}. \tag{24b}$$

We subdivide the integration interval in $N$ equal parts of length

$$h = \frac{2a}{N}, \tag{25}$$

so that

$$\begin{aligned} t_1 &= -a \\ t_{i+1} &= t_i + h \qquad i = 1, \cdots, (N-2). \\ t_N &= a \end{aligned} \tag{26}$$

The differential equation system (23a) ÷ (23b) is, of course, a function of the normalized propagation constant $b$ which is an unknown of the problem, together with the field itself. Therefore we must rely on an iterative procedure, changing the value of $b$ until one is found for which a crossing of the straight line relative to the cover takes place, after $N$ steps (that is for $t = a$). In fact, for any mode, only a value of $b$ exists such that the distance covered on the connecting path equals $2a$. The computer program we have implemented, for performing the required iterations, is very simple and efficient. An optimum accuracy level can be achieved with a computing time that is much shorter than that of other numerical techniques, like the finite element method, previously proposed by other authors. Furthermore, the result can be refined acting, in a really direct way, on the number of subdivisions of the normalized width $2a$.

## III. Numerical Results: TE-Case

With reference to Fig. 1, calculations have been performed for a guide with the following characteristics:

$\lambda_0 = 1.55\ \mu$m,

$2d = 1.\ \mu$m,

$\epsilon_3 = 1.$,

$\epsilon_2 = 11.76$,

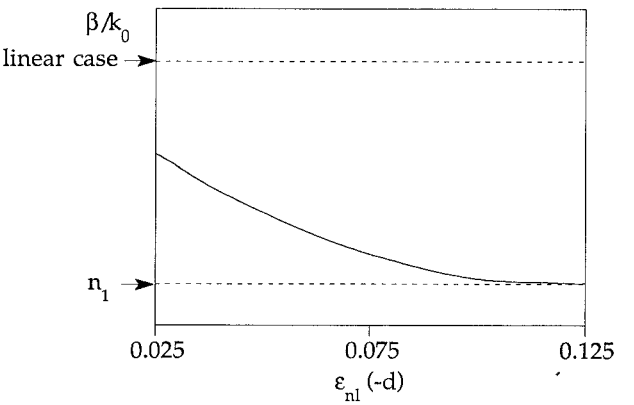


Fig. 7. Dependence of the normalized phase constant $\beta/k_0$ on the parameter $\epsilon_{nl}(-d) = \frac{1}{2}\tau[E_y(-d)]^2$.

and

$\epsilon_1 =$ 11.42, in order to obtain a waveguide which supports only one TE mode,

$\epsilon_1 =$ 10., in order to obtain a waveguide which supports two TE modes,

$\epsilon_1 =$ 7., in order to obtain a waveguide which supports three TE modes.

With the goal of comparing our results with those previously reported in the literature, we have firstly considered a Kerr-type nonlinearity ($\alpha = 2$). In this case, it is convenient, as proposed by other authors [6], [8], to represent the field intensities in terms of the nonlinear dielectric constant change at the interfaces. So we have used the notation $\epsilon_{nl}(-d) = \frac{1}{2}\tau[E_y(-d)]^2$. In Fig. 7 we have drawn the behavior of the normalized phase constant $\beta/k_0$, assuming $\epsilon_{nl}(-d)$ as an independent variable. As expected, the normalized eigenvalue $\beta/k_0$ becomes closer and closer to the refractive index of the cladding region, $n_1 = \sqrt{\epsilon_1}$, when the field at the core-cladding interface increases or, equivalently, when the nonlinearity coefficient $\tau$ is increased as well. This means that the field becomes less and less confined as the time-average power down the guide increases. For $\epsilon_{nl}(-d) = 0.125$ we reach the limit condition, in the sense that no bound mode solution can be found beyond this value. In Fig. 8 we have reported, for the same guide, the near field as a function of the normalized transverse coordinate $x/2d$. Different values of $\epsilon_{nl}(-d)$ are considered, showing, as previously stressed, the confinement reduction effect when this parameter increases. More precisely, the curves have been obtained for a fixed value of the nonlinearity coefficient $\tau$, set equal to $10^{-9}$ m$^2$/V$^2$, while the core-cladding interface field has been made variable. For comparison the result valid in the linear case is also reported in the Figure. It must be noted that field decay in the cover region is much more pronounced that in the cladding region. This is clearly a consequence of the fact that the structure here considered is greatly asymmetric. The curves plotted in Fig. 8 are exactly coincident with those obtainable by the

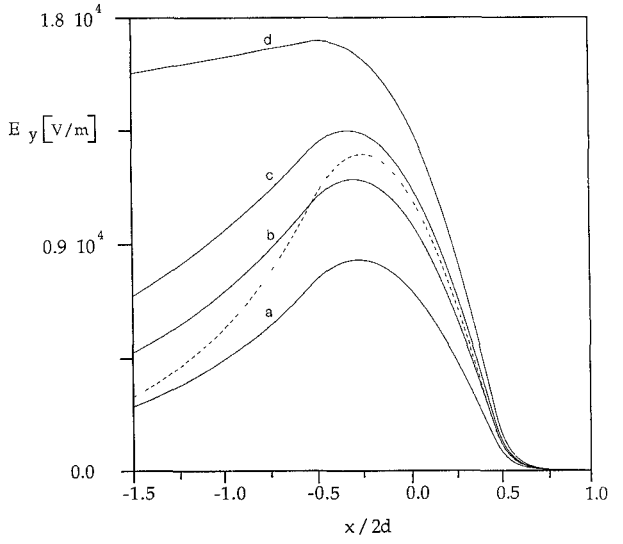


Fig. 8. Waveguide near field profile dependence on the interface field $E_y(-d)$: (a) $E_y(-d) = 0.7 \cdot 10^4$ V/m; (b) $E_y(-d) = 1.0 \cdot 10^4$ V/m; (c) $E_y(-d) = 1.2 \cdot 10^4$ V/m; (d) $E_y(-d) = 1.6 \cdot 10^4$ V/m. In any case the nonlinearity coefficient $\tau$ has been set equal to $10^{-9}$ m$^2$/V$^2$. Dashed line represents the linear case drawn for comparison.

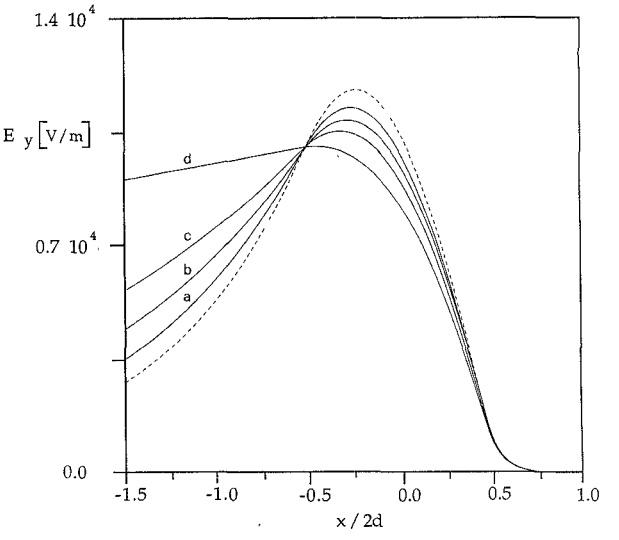


Fig. 9. Waveguide near field profile dependence on the nonlinearity coefficient $\tau$: (a) $\tau = 0.5 \cdot 10^{-9}$ m$^2$/V$^2$; (b) $\tau = 1.0 \cdot 10^{-9}$ m$^2$/V$^2$; (c) $\tau = 1.5 \cdot 10^{-9}$ m$^2$/V$^2$; (d) $\tau = 2.5 \cdot 10^{-9}$ m$^2$/V$^2$. In any case the interface field $E_y(-d)$ has been set equal to $10^4$ V/m. Dashed line represents the linear case drawn for comparison.

completely analytical method described in [8]. This confirms the effectiveness of the procedure here proposed in the case of Kerr-type nonlinearity. At the same time, the validity of [8] is limited to $\alpha = 2$, while the present analysis is much more general and can be applied without limitations on the value of the nonlinearity exponent $\alpha$.

Several other considerations can be made starting from the analysis of Fig. 8. First of all, because of the optical nonlinearity, the field does not increase in proportion with $E_y(-d)$, as it would be usual in the linear case, but it tends to increase more in the cladding and less in the core. At the same time, its maximum shifts towards the core-cladding interface, so confirming the anti-guiding trend as the power flow increases. This consideration suggests, as well known, that the present structure may be used as an optical limiter, directly controllable through the signal level.

If, alternatively, we fix the field value at the core-cladding interface and change the nonlinearity coefficient $\tau$, we obtain the near fields shown in Fig. 9, where we have assumed $E_y(-d) = 10^4$ V/m. In this case, an increase in $\epsilon_{nl}(-d)$ leads to an increase of the field in the cladding region and to a decrease of the field in the core region, with obvious confinement reduction.

Finally, in Fig. 10, the dependence of the field profile on the normalized parameter $a = k_0 d$ is shown, for a fixed value of both the interface fields and $\tau$ (such as to have $\epsilon_{nl}(-d) = 0.05$). When $a$ decreases, that is, $d$ decreases or $\lambda$ increases, the guide exhibits a greater tendency to defocalization. Hence, if we consider that the wavelength has to be chosen on the basis of the material, it is possible to conclude that a reduction in the core width, $d$, leads to a guide that is more sensitive to power fluctuations. The curves of Fig. 10 are quite similar to the analogous ones reported in [8], so confirming, once again, the validity of

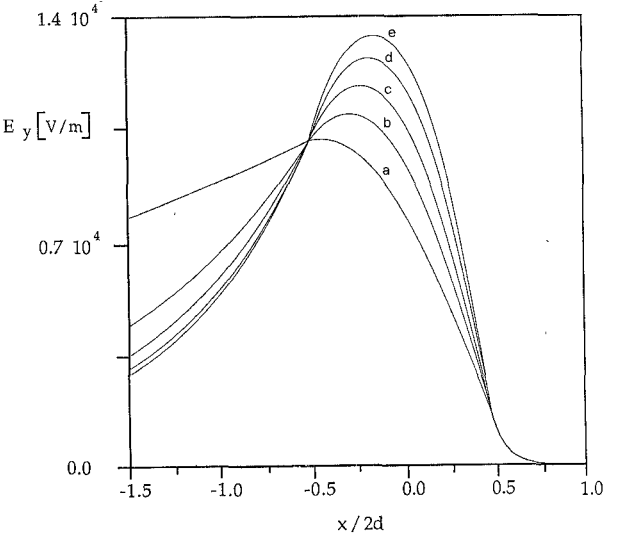


Fig. 10. Waveguide near field profile dependence on the normalized parameter $a$: (a) $a = 3$; (b) $a = 4.05$; (c) $a = 5$; (d) $a = 6$; (e) $a = 7$. The parameter $\epsilon_{nl}(-d)$ has been set equal to 0.05.

the proposed method when applied to already known structures.

On the other hand, one of the main characteristics of the numerical method we have adopted is that it applies to any kind of power-law nonlinearity; so the exponent $\alpha$ can assume any positive value. Assuming $\epsilon_1 = 11.42$, $\epsilon_2 = 11.76$ and $\tau = 10^{-9}$ m$^\alpha$/V$^\alpha$, we have reported in Fig. 11 the maximum field value as a function of the nonlinearity exponent $\alpha$. It has been derived by taking into account that for the asymmetric waveguide under consideration, the fundamental mode is at cut-off, at least in the linear case, when the core-cladding dielectric step is less than about 0.09 [8].

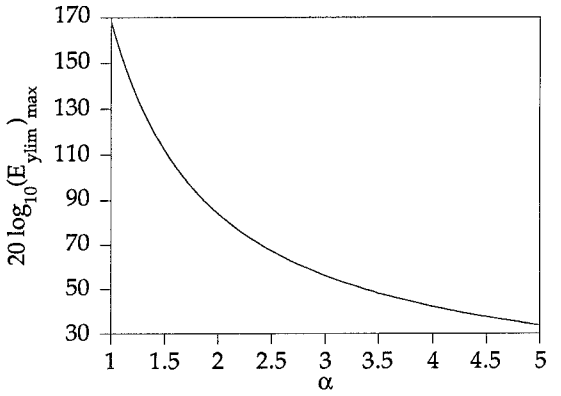


Fig. 11. Maximum field value for the fundamental mode against the nonlinearity exponent $\alpha$.

Therefore, the expression

$$(E_{y\,\mathrm{limit}})_{\max} \approx \left(\frac{\epsilon_2 - \epsilon_1 - 0.09}{\tau}\right)^{1/\alpha} \tag{27}$$

can be considered as a good approximation also in the nonlinear case, whichever the value of $\alpha$ is.

The curve of Fig. 11 is useful in order to make a comparison between types of nonlinearity that differ in the value of the nonlinearity exponent. In Fig. 12, for example, we have drawn the behavior of $E_y$ for some typical values of the parameter $\alpha$. The field at the core-cladding interface has been set equal to 80 V/m, in order to ensure that, for the same values of $\epsilon_1$, $\epsilon_2$ and $\tau$ considered in Fig. 11, the field is bounded also for $\alpha = 4$. Only the field in a significant portion of the core region has been represented, while, externally it decays with the usual exponential law. The curves relative to the values $\alpha = 1$, $\alpha = 2$ and $\alpha = 3$ are practically superimposed because the intensity is too low for an appreciable deviation from linearity to take place. Only in the cases of $\alpha = 3.5$ and $\alpha = 4$ the nonlinearity is large enough to show clearly its effect on the field, whose maximum shifts, at the same time, towards the cladding region.

For the same values of the parameters, we have drawn, in Fig. 13, the normalized phase constant $\beta/k_0$ versus the nonlinearity exponent $\alpha$. Only in the case of $\alpha = 4$ we have a significant reduction in the phase constant value. Again, this is a consequence of the value assumed for the core-cladding interface field. Correspondingly, the mode is almost at the guiding limit and it decays very slowly in the outer regions.

Finally, in Fig. 14, we have reported the field behavior for the three modes, $TE_0$, $TE_1$ and $TE_2$ of a guide with $\epsilon_1 = 7$, $E_y(-d) = 10^4$ V/m, $\alpha = 2$ and $\tau = 10^{-9}$ m$^2$/V$^2$. The numerical values are in perfect agreement with those obtained by the qualitative analysis in the phase-plane. Furthermore, it must be noted that the field distributions are only slightly asymmetric. Obviously, this is a consequence of the particular values we have set for the guide parameters, combined with the strength, not very pronounced, of the nonlinearity assumed.

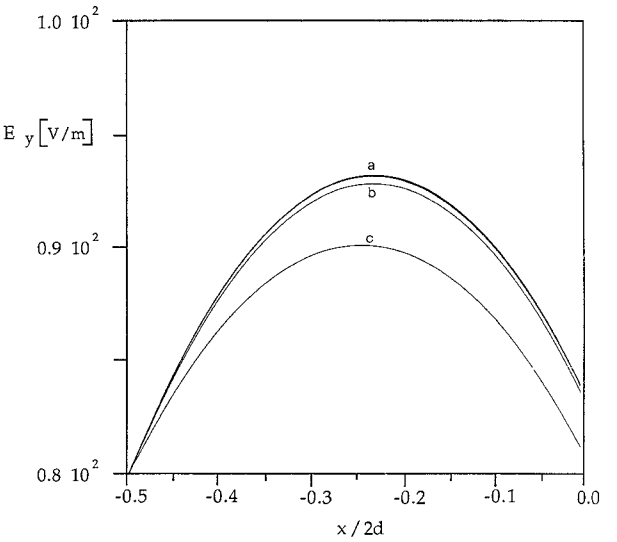


Fig. 12. Waveguide near field profile in a significant portion of the core region for different values of the exponent $\alpha$. Curve (a) refers to the $\alpha$ = 1, 2, 3 cases, which are practically superimposed; curve (b) refers to $\alpha$ = 3.5 and curve (c) to $\alpha = 4$. The interface field $E_y(-d)$ has been set equal to 80 V/m while $\tau = 10^{-9}$ m$^\alpha$/V$^\alpha$.

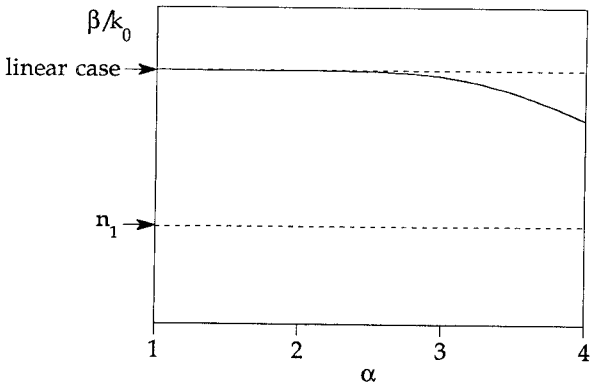


Fig. 13. Normalized phase constant $\beta/k_0$ against the nonlinearity exponent $\alpha$, with $E_y(-d) = 80$ V/m and $\tau = 10^{-9}$ m$^\alpha$/V$^\alpha$.

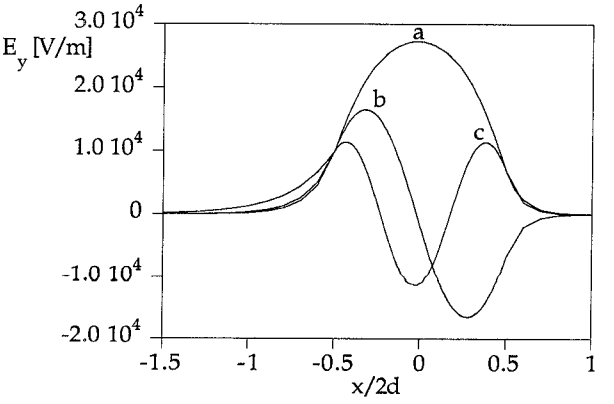


Fig. 14. Electric field distributions of a waveguide which supports three TE modes: (a) $TE_0$; (b) $TE_1$; (c) $TE_2$.

## IV. Theory: TM-Case

This follows lines analogous to the TE case, but with a slightly more complex wave equation, that is now written for the $H_y$ component.

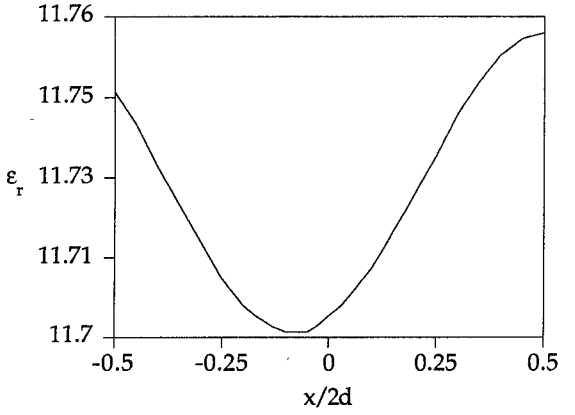


Fig. 15. Behavior of the $\epsilon_r$ in the core for the TM polarization.

In the core, the latter takes the form

$$\frac{d}{dx}\left(\frac{1}{\epsilon_{rz}}\frac{d}{dx}\right)H_{y2} + \left(k_0^2 - \frac{\beta^2}{\epsilon_{rx}}\right)H_{y2} = 0 \qquad (28)$$

where $\epsilon_{rx}$ and $\epsilon_{rz}$ denote the components of the permittivity tensor along $x$ and $z$ respectively, that are functions of $E_{x2}$ and $E_{z2}$.

We consider the electrostrictive case, i.e., $\epsilon_{rx} = \epsilon_{rz} = \epsilon_r$.

Renouncing to define normalized quantities, we set

$$u_2 = H_{y2} \qquad (29a)$$

$$v_2 = \frac{1}{\epsilon_r}\frac{du_2}{dx} \qquad (29b)$$

and express $\epsilon_r$, as a function of $u_2$ and $v_2$ in the core, in the form:

$$\epsilon_r^{\alpha+1} + \epsilon_r^{\alpha}(\theta|v_2|^{\alpha} - \epsilon_2) + \theta\beta^{\alpha}|u_2|^{\alpha} = 0 \qquad (30)$$

where $\theta = \tau/\omega^{\alpha}\epsilon_0^{\alpha}$.

It is noted that, unlike in the TE case, the substitution of (29) in (28) is not sufficient for producing the analytical expression of a locus in phase-plane. This is due to the $\epsilon_r$ dependence on $u_2$ and $v_2$, expressed by (30), which has to be solved at each step of the Runge–Kutta method. In other terms, (30) constitutes a sort of self-consistence condition that the field distribution must satisfy together with (28). As a result, we obtain a semi-analytical expression, not written here for the sake of brevity, which can be managed by simple numerical methods, so allowing us to plot the locus in phase-plane. As an example, we have reported in Fig. 15 the behavior of the $\epsilon_r$ in the core and in Fig. 16 the corresponding locus in phase-plane for the fundamental mode, assuming the following parameter values: $\lambda_0 = 1.55\ \mu$m, $2d = 1\ \mu$m, $\epsilon_1 = 10$, $\epsilon_2 = 11.76$, $\epsilon_3 = 1$, $H_y(-d) = 10^2$ A/m, $\alpha = 2$, $\tau = 10^{-9}$ m$^2$/V$^2$.

The field distributions of the fundamental TM mode are reported in Fig. 17. We note the presence of the required discontinuity in $E_x$ at the dielectric interfaces, whereas $E_z$ and $H_y$ are continuous there.

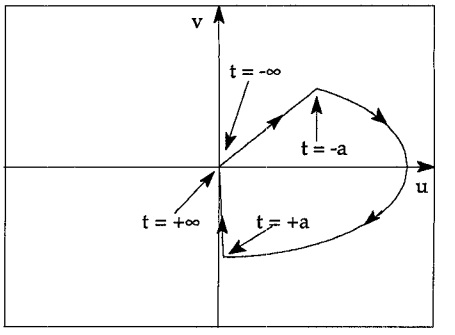


Fig. 16. Sketch of a typical orbit for the fundamental TM mode.

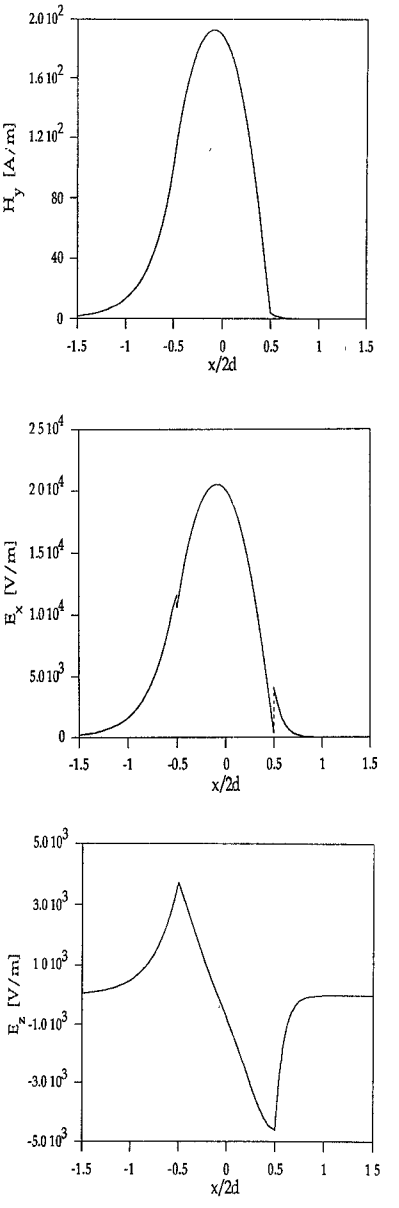


Fig. 17. Field components in the slab for the fundamental TM mode.

## V. Extension to More Complex Structures

The theory described in the previous sections can be extended, without any conceptual difficulty, to consider more practical or more complex cases, such as the guide

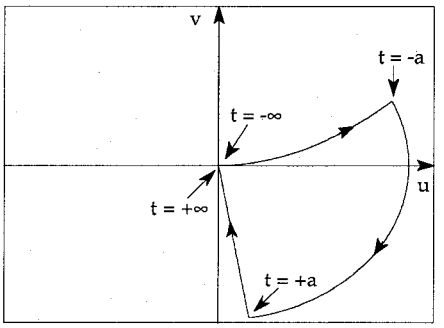


Fig. 18. Sketch of a typical orbit for the fundamental mode of a slab with Kerr-type nonlinearity in the core and in the cladding, assuming the following parameter values: $\lambda_0 = 1.55\ \mu$m, $2d = 1\ \mu$m, $\epsilon_1 = 11.42$, $\epsilon_2 = 11.76$, $\epsilon_3 = 1$, $E_y(-d) = 1.0 \cdot 10^4$ V/m, $\alpha_1 = \alpha = 2$, $\tau_1 = \tau = 1.0 \cdot 10^{-9}$ m$^2$/V$^2$.

with nonlinear cladding. In the latter situation, with reference, for example, to TE polarization, (1a) has to be replaced by

$$\frac{d^2E_{y1}}{dx^2} + (k_0^2\epsilon_1 \pm k_0^2|\tau_1|\,|E_{y1}|^{\alpha_1} - \beta^2)E_{y1} = 0$$
$$-\infty < x \leq -d \tag{31}$$

where the possibility of having a defocusing nonlinearity $(-)$ or a focusing one $(+)$ has been taken into account. By considering the normalized quantities (2) and the asymptotic conditions (5), the locus equation on the $uv$-plane, in the defocusing case becomes

$$v_1^2 - k_1^2u_1^2 - \frac{2}{\alpha_1 + 2}u_1^2|u_1|^{\alpha_1} = 0 \tag{32}$$

which reduces to (7) in the linear case ($\alpha_1 \to -\infty$).

An example of complete locus is shown in Fig. 18, where, again, a Kerr-type nonlinearity has been considered, with the following parameter values: $\lambda_0 = 1.55\ \mu$m, $2d = 1\ \mu$m, $\epsilon_1 = 11.42$, $\epsilon_2 = 11.76$, $\epsilon_3 = 1$, $E_y(-d) = 1.0 \cdot 10^4$ V/m, $\alpha_1 = \alpha = 2$, $\tau_1 = \tau = 1.0 \cdot 10^{-9}$ m$^2$/V$^2$, where $\alpha$ and $\tau$ have the meaning introduced in the previous sections.

The unknown value of $\beta$ and the corresponding field distributions result, as before, from the application of an iterative Runge–Kutta method. Among the infinite possible paths the only one satisfying both the interface conditions has to be found.

In reality, the proposed method is a very general one, so that many other structures, including the TM case with general nonlinearities, for which $\epsilon_{rx} \neq \epsilon_{rz}$, can be studied in the same way, at the expense of a slightly more complicated analysis.

## VI. Conclusion

Introducing phase-plane concepts helps the search for solutions of the nonlinear slab problem in two ways: 1) by restricting the range of possible solutions; 2) by providing a physical interpretation of the results by means of "integrals of motion" in phase-plane.

Current work is directed towards applying these concepts to more realistic three dimensional waveguides.

## References

[1] T. E. Rozzi, "Modal analysis for nonlinear processes in optical and quasi-optical waveguides," *IEEE J. Quantum Electron.*, vol. QE-6, pp. 539–546, Sept. 1970.

[2] S. E. Miller, "Integrated optics: An introduction," *Bell. Syst. Tech. J.*, vol. 48, pp. 2059–2078, Sept. 1969.

[3] A. A. Maradudin, "Nonlinear surface electromagnetic waves," in *Optical and Acoustic Waves in Solids—Modern Topics*, M. Borissov, Ed., Singapore: World Scientific Publ., 1983, pp. 72–142.

[4] G. I. Stegeman, C. T. Seaton, W. M. Heterington III, A. D. Boardman, and P. Egan, "Nonlinear guided waves," in *Nonlinear Optics: Materials and Devices*, C. Flytzanis and J. L. Oudar, Eds., Berlin Heidelberg: Springer-Verlag, 1986, pp. 31–64.

[5] G. I. Stegeman, "Guided wave approach to optical bistability," *IEEE J. Quantum Electron.*, vol. QE-18, pp. 1610–1619, Oct. 1982.

[6] A. D. Boardman and P. Egan, "Optically nonlinear waves in thin films," *IEEE J. Quantum Electron.*, vol. QE-22, pp. 319–324, Feb. 1986.

[7] K. Ogusu, "TE waves in a symmetric dielectric slab waveguide with a Kerr-like non-linear permittivity," *Opt. Quantum Electron.*, vol. 19, pp. 65–72, Jan. 1987.

[8] P. M. Lambkin, K. A. Shore, "Asymmetric semiconductor waveguide with defocusing nonlinearity," *IEEE J. Quantum Electron.*, vol. 24, pp. 2046–2051, Oct. 1988.

[9] K. Hayata, M. Nagai, and M. Koshiba, "Finite-element formalism for nonlinear slab-guided waves," *IEEE Trans. Microwave Theory Tech.*, vol. 36, pp. 1207–1215, July 1988.

[10] K. Ogusu, "TM waves guided by nonlinear planar waveguides," *IEEE Trans. Microwave Theory Tech.*, vol. 37, pp. 941–946, June 1989.

[11] L. Leine, Ch. Wachter, U. Langbein, and F. Lederer, "Propagation phenomena of nonlinear film-guided waves: A numerical analysis," *Opt. Lett.*, vol. 11, pp. 590–592, Sept. 1986.

[12] P. J. Bushell, "Ordinary differential equations," in *Handbook of Applicable Mathematics*, W. Ledermann, Ed., New York: Wiley, 1982, pp. 249–316.

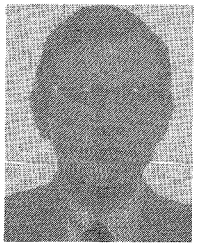

**Tullio Rozzi** (M'66–SM–74–F'90) obtained the degree of 'Dottore' in physics from the University of Pisa in 1965, and the Ph.D. degree in electronic engineering from Leeds University in 1968. In June 1987 he received the degree of D.Sc. from the University of Bath, Bath, U.K.

From 1968 to 1978 he was a Research Scientist at the Philips Research Laboratories, Eindhoven, the Netherlands, having spent one year, 1975, at the Antenna Laboratory, University of Illinois, Urbana. In 1975 he was awarded the Microwave Prize by the IEEE Microwave Theory and Techniques Society. In 1978 he was appointed to the Chair of Electrical Engineering at the University of Liverpool and was subsequently appointed to the Chair of Electronics and Head of the Electronics Group at the University of Bath, in 1981. From 1983 to 1986 he held the additional position of Head of the School of Electrical Engineering at Bath. Since 1988 Dr. Rozzi has been Professor of Antennas in the Department of Electronics and Control, University of Ancona, Italy, while remaining a Visiting Professor at Bath University.

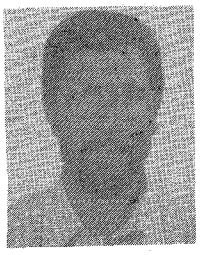

**Franco Chiaraluce** was born in Ancona, Italy, in 1960. He received the degree in Electronic Engineering from the University of Ancona in 1985.

Since 1987 he has been with the Department of Electronics and Automatics at the University of Ancona, where was involved in the field of microstrip antennas and integrated optics. His actual research is mainly devoted to optical communications, semiconductor laser devices and systems.

**Leonardo Zappelli** was born in Rome in 1962. He received the "Doctor" degree in electronic engineering from the University of Ancona, Italy, in 1987.

Since 1988 he has been with the Department of Electronics and Automatics at the University of Ancona, Italy, as a Research Assistant. His research interests are integrated optics and microwaves.